SEMARAK ILMU PUBLISHING

CFD Letters

Journal homepage:
https://semarakilmu.com.my/journals/index.php/CFD_Letters/index
ISSN: 2180-1363

A comparative numerical study of three similar passive solar stills: Single slope, V-type, and greenhouse

Nguyen Van Dung[1], Nguyen Minh Phu[1,*]

[1] Faculty of Heat and Refrigeration Engineering, Industrial University of Ho Chi Minh City, Vietnam

ARTICLE INFO

Article history:
Received 7 April 2023
Received in revised form 10 May 2023
Accepted 15 June 2023
Available online 5 December 2023

Keywords:
Desalination; Solar distillation; Double slope; Symmetry

ABSTRACT

In this paper, three solar stills with similar geometries are numerically investigated for analysis and comparison. The solar stills include single slope, V-type, and greenhouse stills. Steady-state laminar flow numerical simulations with different water surface temperatures and cover glass temperatures are performed. Simulation results were confirmed with data from analytical and experimental models to ensure reliability. The results showed that the V-type still has a higher number of recirculation zones than that of single slope and greenhouse stills. These vortex regions are small, but the velocity magnitude is no less than the other two stills. This difference makes the freshwater yield and convection heat transfer coefficient of V-type still the largest. Daily freshwater productions of single slope, V-type, and greenhouse stills are 0.592, 0.673, and 0.623 kg/m^2, respectively. Productivity at 15 PM is 2.5 times higher than the hours from noon to 14 PM. The natural convection heat transfer coefficient seemed to be unvaried with the temperature difference but changed strongly with the still geometry.

1. Introduction

Freshwater is an essential need of humans, animals, and organisms to sustain life. However, most of the water on earth is saltwater. There is a shortage of potable water in remote areas, and islands in the summer [1]. While these regions are often hot due to high solar radiation [2]. Therefore, using solar energy to produce freshwater is the optimal solution. Passive solar still is a simple and effective device for the hard areas mentioned above [3]. As it is composed of a transparent cover, water basin, and insulation. Passive solar still consists of two types: single slope and double slope. Depending on the layout of the glass covers, the double slope still includes two kinds: V-type and greenhouse. Studying the configurations of passive solar distillation remains a great interest of scientists to improve its productivity [4-7].

Analytical and experimental research for V-type solar still was done early [8, 9]. However, a numerical investigation to analyze the heat and mass transfer phenomena in the still enclosure has not been found. Rahbar *et al.,* [10, 11] confirmed that computational fluid dynamics (CFD) is a good

* *Corresponding author.*
E-mail address: nguyenminhphu@iuh.edu.vn (Nguyen Minh Phu)

https://doi.org/10.37934/cfdl.16.1.6878

tool for explaining transport phenomena in a solar still. Edalatpour *et al.,* [12] placed baffles in the still chamber to change the natural convection flow pattern. They have drawn that baffle location can either increase or decrease freshwater yield. Rashidi *et al.,* [13] added nanoparticles to a single-slope solar still. The results show an increase in productivity of up to 25%. Keshtkar *et al.,* [14] examined numerically to compare the yield of three solar stills including single slope, greenhouse, and multi-stage greenhouse stills. The yields of these stills were 5.652 kg/m^2, 11.82 kg/m^2, and 24.3 kg/m^2, respectively. Chen *et al.,* [15] studied the floating greenhouse still by outdoor experiment and numerical simulation approaches. The highest yield of 1.5 kg/m^2 was achieved in their study. Recently, Shoeibi *et al.,* [16] used nanofluid to cool the cover glass of a greenhouse still. They reported that freshwater yield increased by 11.09% compared to the still without nanopowders.

Single slope, V-type, and greenhouse solar stills have similar shapes. However, a comparative study of the yield and transport phenomena of these three types was not found. In addition, numerical research for V-type still has been lacking attention. To bridge these gaps, simulation of three still enclosures was performed in this study. The two-dimensional (2D) computational domain and symmetric boundary conditions are used to reduce the computation time for these similar stills. The influence of hourly boundary temperatures on yield and transport mechanism was investigated and analyzed.

2. Model Description

Figure 1 shows three similar passive solar stills including single slope (SS), V-type and greenhouse distiller. The SS still is the most conventional and simple. The V-type still has a condensate trap in the middle. While the greenhouse still has 2 traps placed on either side. It is conceivable that the V-type and greenhouse stills are composed of two SS stills symmetrically assembled from the short vertical edge and the long vertical edge, respectively. In other words, V-type or greenhouse stills is equivalent to two individual SS stills. Hence 3 stills are simulated from a computational domain with different boundary conditions as shown in Figure 2. The calculation domain has dimensions of short vertical edge h_l = 75 mm, long vertical edge h_r = 187 mm, water surface length L = 438 mm, and glass inclination θ = 14.35° [11]. Simulation of the computational domain is performed with the following assumptions:

- Laminar, two-dimensional, and time-independent flow,
- Fluid is moist air,
- The thermophysical parameters of humid air are calculated as in Table 1.
- Ignore the effect of thermal radiation.

Table 1
Models for the thermophysical properties [17]

Property	Model
Density	Incompressible ideal gas
Specific heat capacity	Mixing law
Thermal conductivity and viscosity	Mass-weighted mixing law
Thermal diffusion coefficient	Kinetic theory

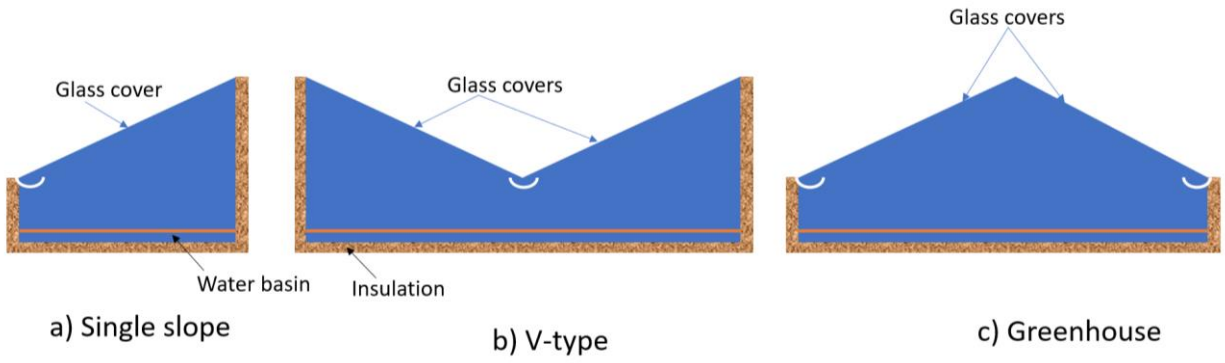

Fig. 1. Three similar passive solar stills

Based on the assumptions, the governing equations can be written as:

The continuity equation [18, 19]:

$$\frac{\partial u}{\partial x}+\frac{\partial v}{\partial y}=0 \tag{1}$$

where *u* is the horizontal velocity component, *v* is the vertical velocity component, *x* and *y* are Descartes coordinates.

x-momentum equation:

$$u\frac{\partial u}{\partial x}+v\frac{\partial u}{\partial y}=-\frac{1}{\rho}\frac{\partial p}{\partial x}+\nu\left(\frac{\partial^2 u}{\partial x^2}+\frac{\partial^2 u}{\partial y^2}\right) \tag{2}$$

where *p* is pressure, ρ is density, and ν is kinematic viscosity.

y-momentum equation [20]:

$$u\frac{\partial v}{\partial x}+v\frac{\partial v}{\partial y}=-\frac{1}{\rho}\frac{\partial p}{\partial y}+\nu\left(\frac{\partial^2 v}{\partial x^2}+\frac{\partial^2 v}{\partial y^2}\right)+g \tag{3}$$

where *g* is the gravity acceleration.

Energy equation:

$$u\frac{\partial T}{\partial x}+v\frac{\partial T}{\partial y}=\alpha\left(\frac{\partial^2 T}{\partial x^2}+\frac{\partial^2 T}{\partial y^2}\right) \tag{4}$$

where *T* is temperature, and α thermal diffusivity.

Transport equation for the water vapor mass fraction (Y) [15]:

$$u\frac{\partial Y}{\partial x}+v\frac{\partial Y}{\partial y}=D_m\left(\frac{\partial^2 Y}{\partial x^2}+\frac{\partial^2 Y}{\partial y^2}\right) \tag{5}$$

where mass diffusivity (D_m) can be estimated as [14, 21]:

$$D_m=2.6\times10^{-5}\left(\frac{101325}{p}\right)\left(\frac{T}{298}\right)^{1.5} \tag{6}$$

Boundary conditions associated with partial differential equations Eq. (1)-(5) are presented in Figure 2 with the no-slip condition for all boundaries except symmetry walls. Y_g and Y_w are the water vapor mass fractions of saturated humid air at temperatures T_g and T_w, respectively. Figure 3 shows meshing in the computational domain. Dense meshing at water and glass surfaces to enhance flow physics predictions at these surfaces. Many element sizes have been tested to reach grid independence. The results show that the number of elements of 65634 achieves the result stability and suitable calculation time. Distillers were simulated in ANSYS Fluent 19.2 software. The SIMPLE algorithm is used to link pressure and velocity in the Navier-Stokes equations. Species transport model in ANSYS Fluent is employed to simulate the mass fraction of the air-water vapor mixture. The iteration will stop when the error of the energy equation is 10^{-6}, and the other equations of 10^{-3}.

From the simulation results, the freshwater production capacity ($\dot{m}$) calculated for one square meter of water surface in one hour (kg/m^2.h) of a distillation unit is expressed as follows [10, 14]:

$$\dot{m}=\frac{-3600D_m\rho}{L}\int_0^L\left.\frac{\partial Y}{\partial y}\right|_{water\ surface}dx \tag{7}$$

where L is the length of water surface.

And the convection heat transfer coefficient (CHTC) between the water surface and glass cover can be determined by the following equation: .

$$h_c=\frac{-k}{L(T_w-T_g)}\int_0^L\left.\frac{\partial T}{\partial y}\right|_{water\ surface}dx \tag{8}$$

where k is thermal conductivity.

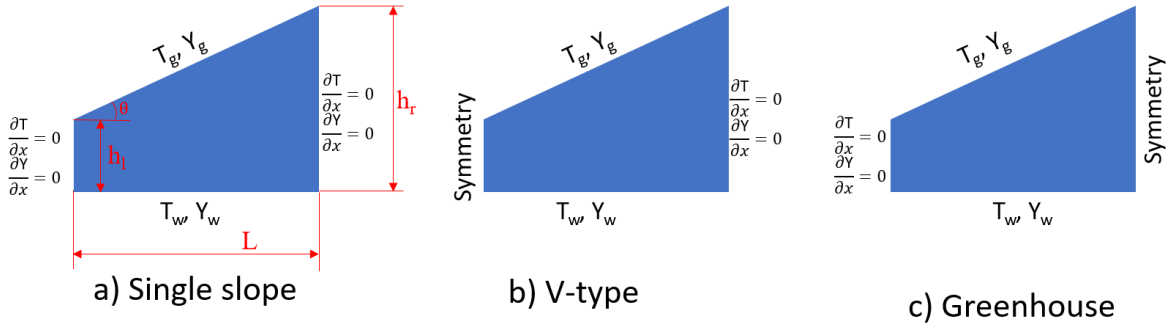

Fig. 2. Computational domain and boundary conditions

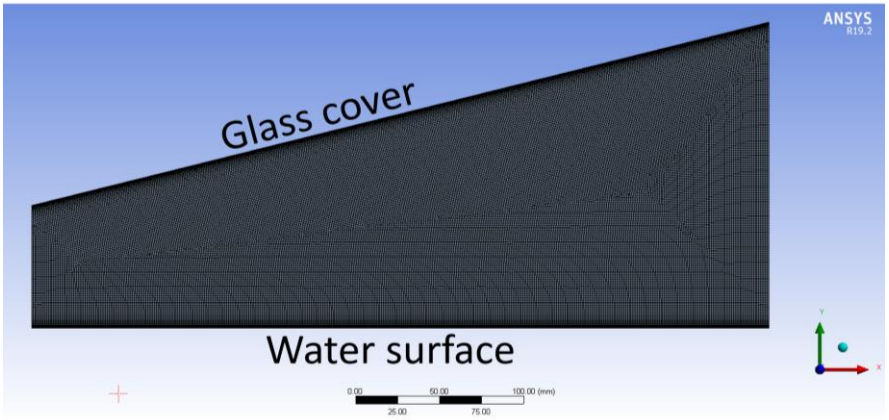

Fig. 3. Mesh generation with refinement at glass cover and water surface

To ensure reliable simulation, the performance of SS still is compared with the prediction of well-known Dunkle's mathematical model and published experimental result in the study of Rahbar and Esfahani [11]. Figure 4 shows the comparison between three approaches. It can be seen that the current calculation result stands between the results from Dunkle's model and the experiment. The simulation is therefore reliable and extended to similar distillers.

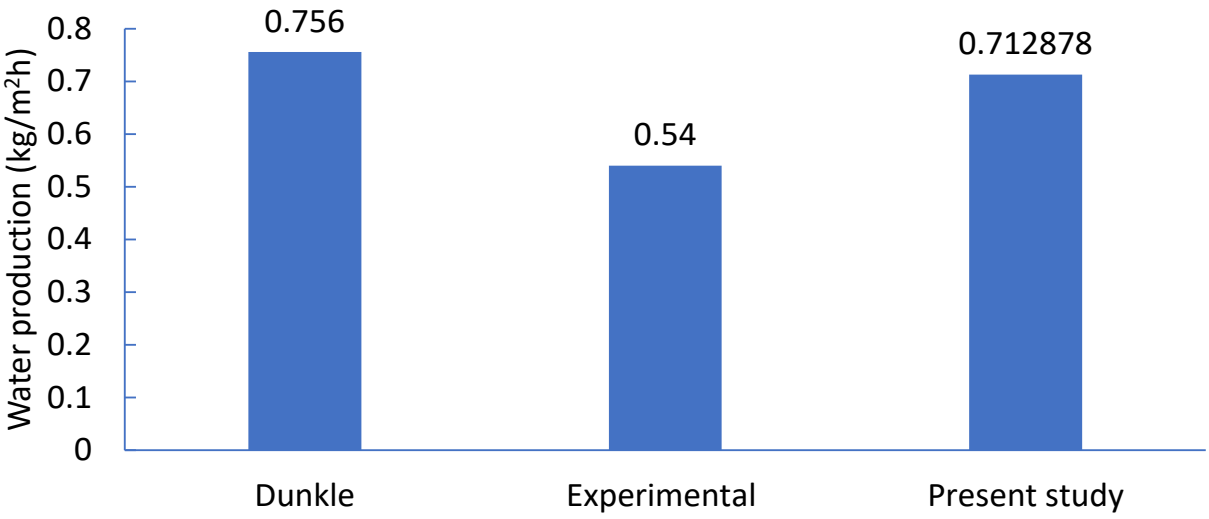

Fig. 4. Comparison of single slope still at T_w = 63°C and T_g = 48°C with the prediction of Dunkle's model and experimental result [11]

3. Results and Discussions

Table 2 presents the hourly glass and water surface temperatures used for the analysis and comparison of the three solar stills in this section. These temperatures are experimental data in the single slope still study of Rashidi *et al.,* [20].

Table 2
Hourly variation of the glass cover and water surface temperatures

Hour	T_w (°C)	T_g (°C)
9	36	36
10	47	46
11	55	53
12	63	61
13	64	62
14	65	63
15	65	61
16	58	54

Figures 5 to 8 visualize heat and fluid flow at 15 PM. This is the time with the highest water surface temperature and the largest temperature difference ($T_w - T_g$). Figure 5 shows the magnitude of the velocity in the stills. The air and water vapor mixture in the greenhouse still has the highest velocity because the free area in the middle is the largest. SS still has the smallest natural convection velocity due to the narrowest space. The fluid velocity on the left edge of the V-type solar still is up to 0.09 m/s. The fluid velocity on the right edge of the greenhouse still is up to 0.13 m/s. Two large vortices in the upper right corner of SS and V-type stills can be observed. These are dead zones that reduce the condensation surface of water vapor. It is worth noting that V-type still produces 4 primary vortices while 2 other stills have 3 primary vortices. Therefore, V-type still may obtain high water production due to increase in rotation [12, 20].

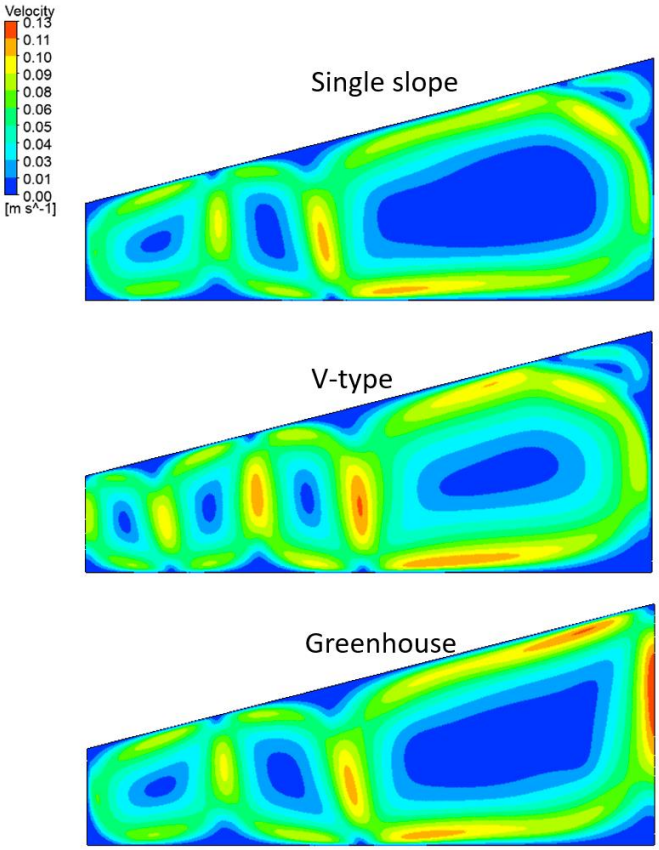

Fig. 5. Contour of velocity magnitude at 15 PM

The vertical convection current is represented by the velocity component v. Figure 6 shows the v-velocity at the y = 50 mm horizontal line. Positive velocity represents upward current and negative velocity represents downward current. The current goes up at roughly the same speed close to the right edge (x = 438 mm) of the three stills. Hence the right vortex is counterclockwise. Successive vortices have the opposite direction as gear meshing. Due to the larger number of vortices of the V-type still, the clockwise vortex occurs close to the symmetry wall of the V-type still (x = 0). Although the number of vortices increases and thus the vortex size is small in the V-type still, the magnitude of v-velocity is not inferior to the remaining 2 stills. Therefore, the intensity of convection heat exchange in the V-type still does not decline.

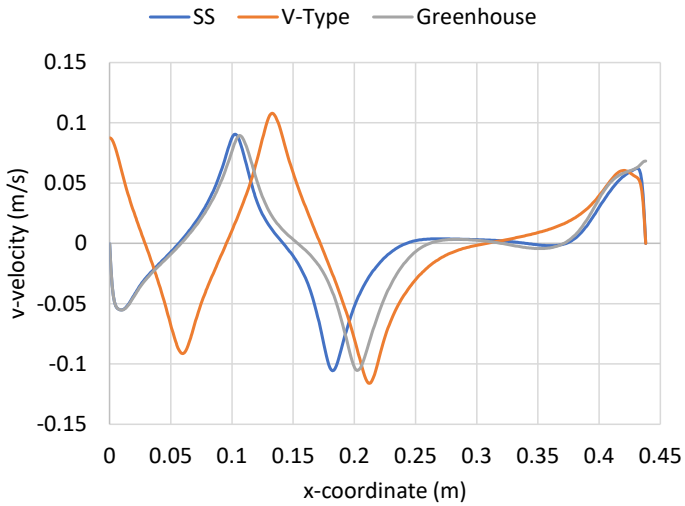

Fig. 6. Variation of v-velocity at the line y = 50 mm

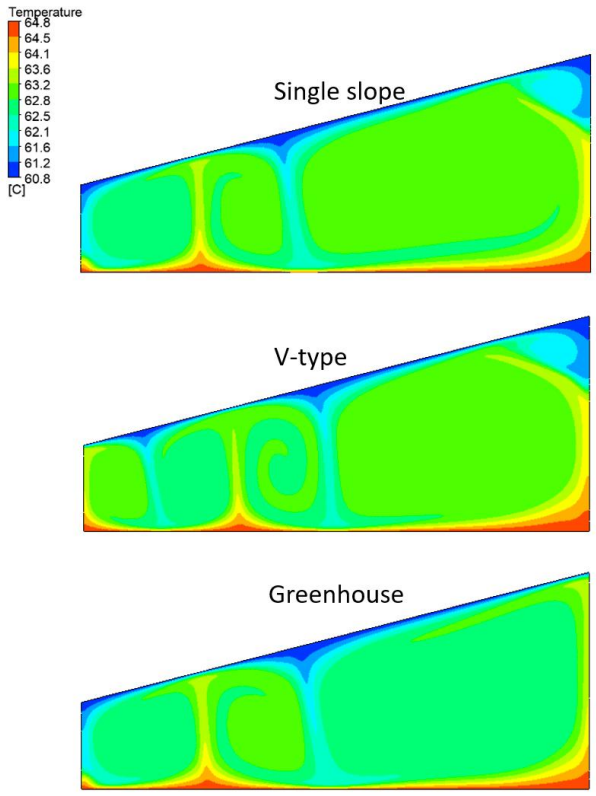

Fig. 7. Temperature distribution inside the solar stills at 15 PM

The temperature distribution in the stills is shown in Figure 7. The temperature in the stills is relatively uniform. But the temperature changes sharply near the water and glass surfaces. Therefore, transport characteristics occur strongly near these surfaces. There is a thermal plume on the water surface with a temperature of 64°C. A thermal plume at glass cover with a temperature of 61.6°C was observed for SS and greenhouse stills. For V-type still, there are 2 thermal plumes at the cover glass due to 4 rotations. The vapor mass fraction distribution is quite like the temperature distribution as shown in Figure 8. Most of the area has a mass fraction of 0.153. This is the average value of the mass fractions at the water and glass surfaces. Due to condensation and evaporation, there is a significant variation of the mass fraction near the glass and the water surface.

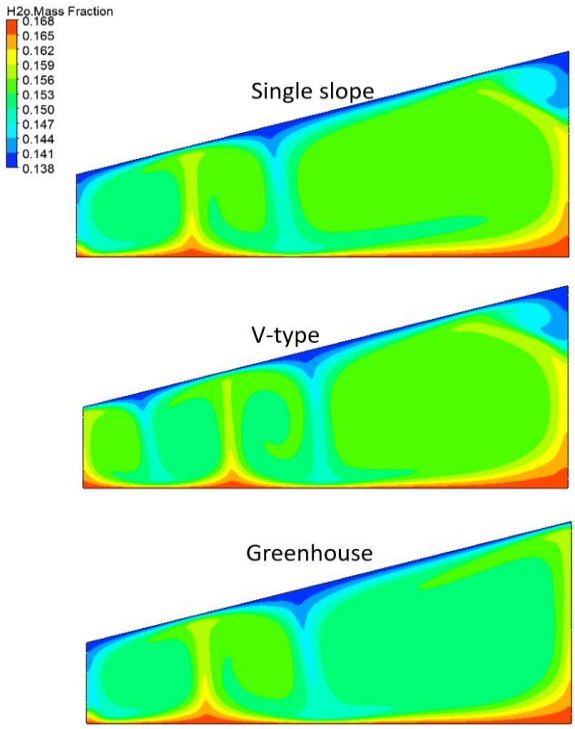

Fig. 8. Water vapor mass fraction inside the solar stills at 15 PM

Hourly freshwater yield is shown in Figure 9. The yield increases with the water surface temperature and the temperature difference between the water surface and the glass. Thus, the yield increases from 9 AM and peaks at 15 PM. At 16 PM, productivity is lower due to reduction of water surface temperature. V-type still achieves the greatest yield due to its four-rotation flow pattern. Greenhouse still obtains the second highest yield due to the high natural convection velocity. Between noon and 14 PM, the yield increased slightly due to the increase in water surface temperature while the temperature difference remained constant. Productivity at 15 PM is 2.5 times higher than previous hours. This is due to the heat storage of the water, so the water surface temperature is very high at 15 PM while the glass temperature has decreased with the ambient temperature. Cumulative freshwater production is seen in Figure 10. At the end of the day, the yields of SS still, V-type still, and greenhouse still are 0.592, 0.673, and 0.623 kg/m^2, respectively. That means the yield of V-type still is higher than that of SS still and greenhouse still 1.13 and 1.08 times, respectively.

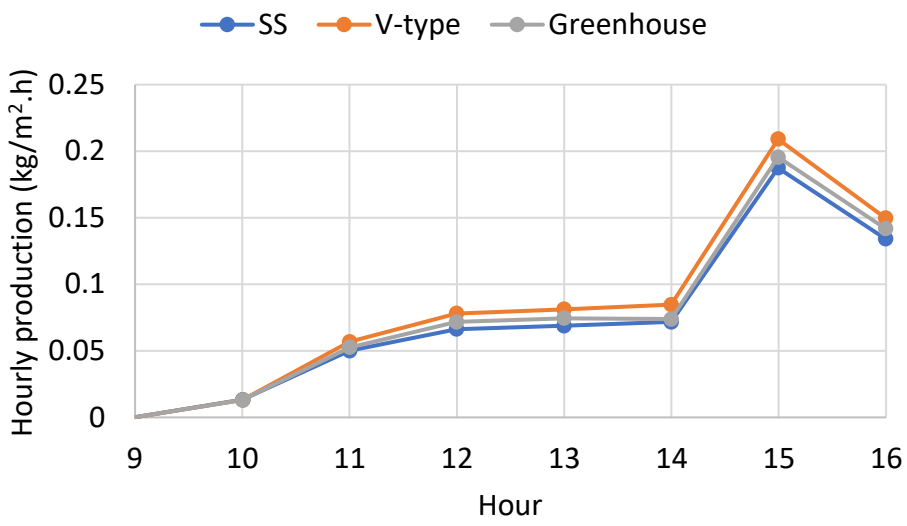

Fig. 9. Hourly water productivity with different stills

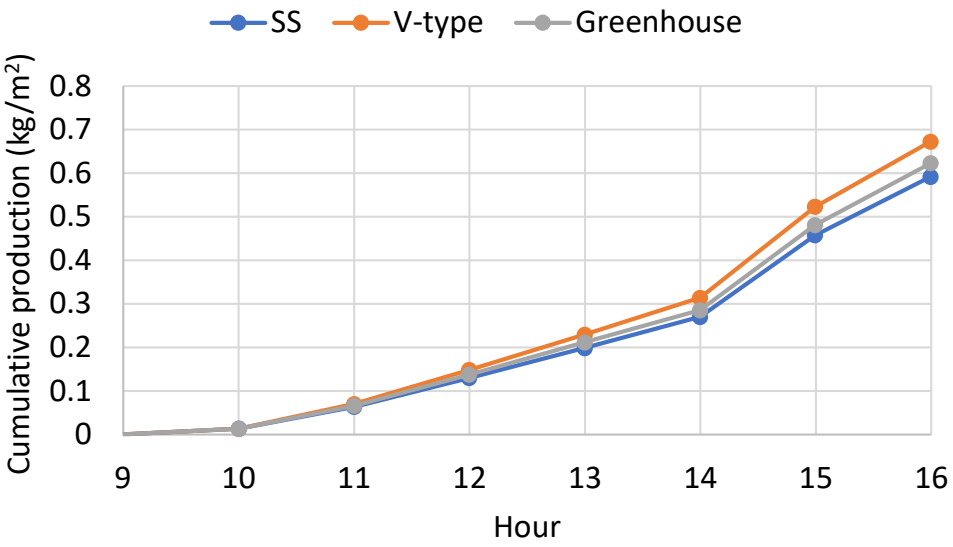

Fig. 10. Cumulative freshwater production with different stills

The convection heat transfer coefficient (CHTC) in stills with time is shown in Figure 11. In general, the natural convection heat transfer coefficient is proportional to the temperature difference [22]. Hence the coefficient of a still is almost constant between 11 AM and 14 PM due to temperature difference of 2 K, like 15 PM and 16 PM with temperature difference of 4 K. On the other hand, the effect of temperature gradient near water surface causes change of CHTC with still shape. V-type still has the largest CHTC due to the 4-vortex structure leading to the highest temperature gradient at the water surface.

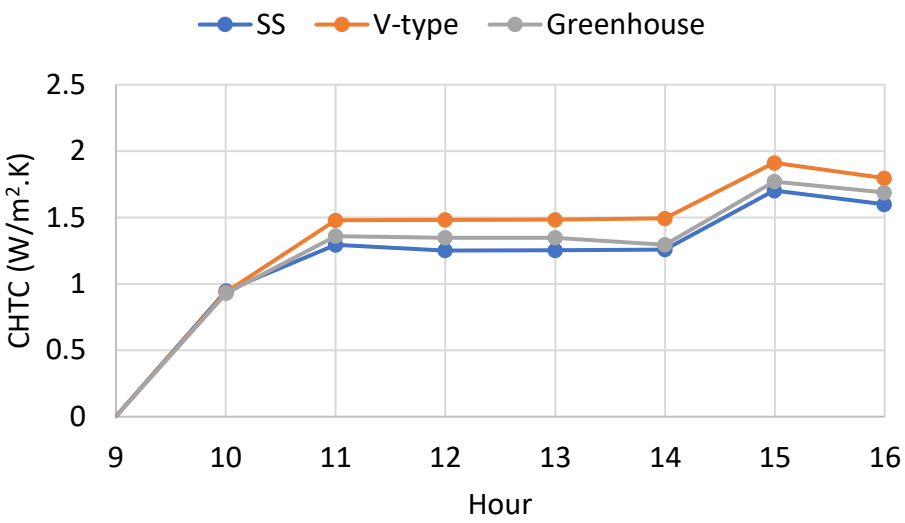

Fig. 11. Hourly convective heat transfer coefficient with different stills

4. Conclusions

2D numerical simulations for single slope, V-type, and greenhouse solar stills were performed in this study. These three types have similar shapes derived from a right trapezoid. Therefore, they are simulated simultaneously to compare productivity, heat transfer coefficient and flow fields. The main results are drawn as follows:

- The number of swirls in V-type still is greater than that of single slope and greenhouse stills.
- The amount of drinking water collected per day of single slope, V-type, and greenhouse solar stills is 0.592, 0.673, and 0.623 kg/m^2, respectively.
- Natural convection velocity in greenhouse solar still is the largest followed by V-type still.
- For the same temperature difference, the convective heat transfer coefficient of V-type distiller is the largest followed by greenhouse solar still.
- Fresh water productivity at 15 PM is 2.5 times higher than that at noon, 13 PM, or 14 PM.

Acknowledgement

This research was not funded by any grant.

References

[1] Rabhy, Omar O., I. G. Adam, M. Elsayed Youssef, A. B. Rashad, and Gasser E. Hassan. "Numerical and experimental analyses of a transparent solar distiller for an agricultural greenhouse." *Applied Energy* 253 (2019): 113564. https://doi.org/10.1016/j.apenergy.2019.113564

[2] Voa, Kien Quoc, Chi Hiep Lea, and An Quoc Hoangb. "Optimization of mass flow rate ratio of water and air in humidification–dehumidification desalination systems." *Desalination and Water Treatment* 246 (2022): 82-91. https://doi.org/10.5004/dwt.2022.28034

[3] Hồ, Huy Đăng, and Viết Văn Hoàng. "Thermal analysis of water distillation system using pv/t collector combined single basin still." *VNUHCM Journal of Engineering and Technology* 5, no. 4 (2022): 1661-1678. https://doi.org/10.32508/stdjet.v5i4.1033

[4] Rashid, Farhan Lafta, Abbas Sahi Shareef, and Hasan Fathi Alwan. "Enhancement of fresh water production in solar still using new phase change materials." *Journal of Advanced Research in Fluid Mechanics and Thermal Sciences* 61, no. 1 (2019): 63-72.

[5] Mugisidi, Dan, Berkah Fajar, Syaiful Syaiful, Tony Utomo, Oktarina Heriyani, Delvis Agusman, and Regita Regita. "Iron Sand as a Heat Absorber to Enhance Performance of a Single-Basin Solar Still." *Journal of Advanced Research in Fluid Mechanics and Thermal Sciences* 70, no. 1 (2020): 125-135. https://doi.org/10.37934/arfmts.70.1.125135

[6] Haddad, Zakaria, Abla Chaker, Azzedine Nahoui, Mohamed Salmi, and Islam Laifa. "Experimental Study of an Inclined Wick Solar Still Operating in Drop by Drop System Under The Climatic Conditions of Hodna's Region, Algeria." *Journal of Advanced Research in Fluid Mechanics and Thermal Sciences* 94, no. 1 (2022): 188-199. https://doi.org/10.37934/arfmts.94.1.188199

[7] Nahoui, Azzedine, Redha Rebhi, Giulio Lorenzini, and Younes Menni. "Numerical study of a basin type solar still with a double glass cover under winter conditions." *Journal of Advanced Research in Fluid Mechanics and Thermal Sciences* 88, no. 1 (2021): 35-48. https://doi.org/10.37934/arfmts.88.1.3548

[8] Nahoui, Azzedine, Redha Rebhi, Giulio Lorenzini, and Younes Menni. "Numerical study of a basin type solar still with a double glass cover under winter conditions." *Journal of Advanced Research in Fluid Mechanics and Thermal Sciences* 88, no. 1 (2021): 35-48.

[9] Suneesh, P. U., R. Jayaprakash, T. Arunkumar, and David Denkenberger. "Effect of air flow on "V" type solar still with cotton gauze cooling." *Desalination* 337 (2014): 1-5.https://doi.org/10.1016/j.desal.2013.12.035

[10] Rahbar, Nader, Amin Asadi, and Ehsan Fotouhi-Bafghi. "Performance evaluation of two solar stills of different geometries: tubular versus triangular: experimental study, numerical simulation, and second law analysis." *Desalination* 443 (2018): 44-55.https://doi.org/10.1016/j.desal.2018.05.015

[11] Rahbar, Nader, and Javad Abolfazli Esfahani. "Productivity estimation of a single-slope solar still: Theoretical and numerical analysis." *Energy* 49 (2013): 289-297. https://doi.org/10.1016/j.energy.2012.10.023

[12] Edalatpour, Mojtaba, Ali Kianifar, and Shamsoddin Ghiami. "Effect of blade installation on heat transfer and fluid flow within a single slope solar still." *International Communications in Heat and Mass Transfer* 66 (2015): 63-70.https://doi.org/10.1016/j.icheatmasstransfer.2015.05.015

[13] Rashidi, Saman, Shima Akar, Masoud Bovand, and Rahmat Ellahi. "Volume of fluid model to simulate the nanofluid flow and entropy generation in a single slope solar still." *Renewable Energy* 115 (2018): 400-410. https://doi.org/10.1016/j.renene.2017.08.059

[14] Keshtkar, M., M. Eslami, and K. Jafarpur. "A novel procedure for transient CFD modeling of basin solar stills: Coupling of species and energy equations." *Desalination* 481 (2020): 114350. https://doi.org/10.1016/j.desal.2020.114350

[15] Chen, Siliang, Panpan Zhao, Guo Xie, Yuanke Wei, Yijing Lyu, Yingjing Zhang, Tiantong Yan, and Tingting Zhang. "A floating solar still inspired by continuous root water intake." *Desalination* 512 (2021): 115133. https://doi.org/10.1016/j.desal.2021.115133

[16] Shoeibi, Shahin, Hadi Kargarsharifabad, Nader Rahbar, Goodarz Ahmadi, and Mohammad Reza Safaei. "Performance evaluation of a solar still using hybrid nanofluid glass cooling-CFD simulation and environmental analysis." *Sustainable Energy Technologies and Assessments* 49 (2022): 101728. https://doi.org/10.1016/j.seta.2021.101728

[17] Yan, Tiantong, Guo Xie, Hongtao Liu, Zhanglin Wu, and Licheng Sun. "CFD investigation of vapor transportation in a tubular solar still operating under vacuum." *International Journal of Heat and Mass Transfer* 156 (2020): 119917. https://doi.org/10.1016/j.ijheatmasstransfer.2020.119917

[18] Phu, Nguyen Minh, and Nguyen Van Hap. "Numerical Investigation of Natural Convection and Entropy Generation of Water near Density Inversion in a Cavity Having Circular and Elliptical Body." *Computational Overview of Fluid Structure Interaction* 121 (2020). https://doi.org/10.5772/intechopen.95301

[19] Thanh, Luan Nguyen, Phu Nguyen Minh, and Ha Nguyen Minh. "Entropy Generation, Heat Transfer of Water Near Density Inversion Region with Relative Positions of Hot and Cold Walls: Numerical Analysis." *CFD Letters* 15, no. 5 (2023): 42-53. https://doi.org/10.37934/cfdl.15.5.4253

[20] Rashidi, Saman, Javad Abolfazli Esfahani, and Nader Rahbar. "Partitioning of solar still for performance recovery: experimental and numerical investigations with cost analysis." *Solar Energy* 153 (2017): 41-50. https://doi.org/10.1016/j.solener.2017.05.041

[21] Mittal, Gaurav. "An unsteady CFD modelling of a single slope solar still." *Materials Today: Proceedings* 46 (2021): 10991-10995. https://doi.org/10.1016/j.matpr.2021.02.090

[22] Luan, Nguyen Thanh, and Nguyen Minh Phu. "First and second law evaluation of multipass flat-plate solar air collector and optimization using preference selection index method." *Mathematical Problems in Engineering* 2021 (2021): 1-16. https://doi.org/10.1155/2021/5563882